Endocrinology

A New Cell Secreting Insulin

Sib Sankar Roy, Mohua Mukherjee, Samir Bhattacharya, C. N. Mandal, L. Ravi Kumar, Subrata Dasgupta, I. Bandyopadhyay and Katsumi Wakabayashi

Endocrinology 2003 144: 1585-1593, doi: 10.1210/en.2002-220350

0013-7227/03/$15.00/0
Printed in U.S.A.

Endocrinology 144(4):1585–1593

doi: 10.1210/en.2002-220350

A New Cell Secreting Insulin

SIB SANKAR ROY*, MOHUA MUKHERJEE*, SAMIR BHATTACHARYA*, C. N. MANDAL, L. RAVI KUMAR, SUBRATA DASGUPTA, I. BANDYOPADHYAY, AND KATSUMI WAKABAYASHI

Indian Institute of Chemical Biology (S.S.R., M.M., S.B., C.N.M.), Calcutta 700032, India; and School of Life Science, Department of Zoology, Visva Bharati University (L.R.K., S.D., I.B.), Santiniketan 731235, India; and Institute for Molecular and Cellular Regulation, Gunma University (K.W.), Maebashi 371-0847, Japan

The pancreatic β-cell is the only cell in animals that expresses the insulin gene and secretes insulin protein. We have found copious release of immunoreactive and bioactive insulin into the medium from the primary culture of carp adipocytes. Glucose augmented this release to more than 2-fold, and glucose transporter, Glut2, was detected in these cells. These all reflect characteristics of a pancreatic β-cell. The expression of the adipocyte-specific flotillin gene, the presence of peroxisomal proliferator-activated receptor γ and Glut4, and the colocalization of insulin and leptin confirmed the identity of these cells as adipocytes. Purified carp adipocyte insulin (AdpInsl) comigrated with porcine and bovine insulin in SDS-PAGE, indicating the similarity of their molecular sizes (5.5 kDa). AdpInsl strongly reduced hyperglycemia in streptozotocin-induced diabetic rats. It also stimulated significantly higher glucose uptake in carp and hamster adipocytes than porcine insulin. Adipocyte RNA hybridized with rat and zebrafish insulin cDNA showing the expression of the insulin gene in this cell. Using oligonucleotide primers designed on the basis of conserved insulin domain, AdpInsl cDNA was reverse transcribed, cloned, and sequenced. The deduced amino acid sequence of AdpInsl A and B chain exhibited 98% homology with zebrafish and more than 70% homology with human, porcine, and murine insulin. To understand the structure-function relationship between AdpInsl and mammalian β-cell insulin, we have analyzed the amino acid sequences and three-dimensional structure of AdpInsl. In the critical determinant segment for receptor binding, AdpInsl has His at the A8 position instead of Thr in human and porcine insulin, and this attributed greater biological activity to AdpInsl. Our results show that carp adipocyte is a unique cell. As an insulin target cell it can express the insulin gene and secrete highly active insulin protein; thus, it may serve as a natural alternative to pancreatic β-cell insulin. (*Endocrinology* 144: 1585–1593, 2003)

INSULIN GENE expression and secretion of insulin protein in all adult animals, including humans, are still known to be pancreatic β-cell specific. A search for an alternative source of pancreatic β-cells in nature has not yet been successful. Insulin-like material was detected in the bacteria *Escherichia coli* (1), and immunoreactive and bioactive insulin was found in eukaryotes (2), insects, and annelids (3). Extrapancreatic distribution of insulin was reported in rats and humans (4). Cells of endodermal origin in rats expressed the insulin gene during embryonic development (5), but insulin secretion from them is not known. In lower vertebrates such as fish, islet cells may be located in pancreatic or extrapancreatic tissue (6–8), but it is the islet cell that released highly active insulin (6, 9) in a greater amount than mammals on the basis of unit of tissue (10). The structure and function of β-cell insulin in all vertebrates are fairly conserved. The insulin monomer in the majority of cases consists of two polypeptide chains, an A chain of 21 amino acid residues and a B chain of 30 amino acid residues. These two polypeptide chains contain one intrachain (A6-A11) and two interchain (A7-B7 and A20-B19) disulfide linkages. To understand the insulin structure-function relationship, the importance of the N-terminal helix of A chain segment A1-A8 has been recognized for receptor interaction by determining the biological activity for a range of chemical derivatives. In the B chain, B24-B26 has been shown to be involved in receptor-binding activity (11, 12).

We have found that adipocytes from a carp can express the insulin gene and secrete immunoreactive and biologically active insulin. The carp adipocyte insulin (AdpInsl) gene has been cloned; deduced amino acid and peptide structures have been compared with those of β-cell insulin. We have modeled the three-dimensional structure of AdpInsl by homology modeling based on the structure of human insulin (13, 14) to explain our experimental results obtained with AdpInsl.

Abbreviations: AdpInsl, Carp adipocyte insulin; ir-insulin, immunoreactive insulin; PB, permeabilization buffer; PPARγ, peroxisomal proliferator-activated receptor γ; RACE, rapid amplification of cDNA ends; UTR, untranslated region.

Materials and Methods

Adipocyte culture

Cells from fat tissue, liver, and kidney from the carp (*Catla catla*) were isolated and incubated in the following manner. Fat tissue around the small intestine of carp were collected in a petri dish, minced with the help of fine scissors, then transferred to a 50-ml beaker containing MEM (MEM without calcium, Sigma-Aldrich, St. Louis, MO; salinity adjusted to 0.6%) containing collagenase type II (0.6 mg/ml), fatty acid-free 3% BSA fraction V (Sigma-Aldrich). This was incubated at 30 C for 1 h with occasional stirring. On termination of the incubation, the beaker was placed at 42 C in a water bath for 10 min, followed by a rapid filtration through tightly meshed nylon cloth. Cells were washed with MEM-EDTA, and the viability of the cells was determined by the exclusion of trypan blue dye (0.1%). No mortality was observed until 10 h of incubation (Fig. 1). Cells were incubated with Ca^{2+}-free MEM (5.5 mM glucose) containing 25 mM HEPES, 100 IU/ml penicillin, 100 μg/ml streptomycin, and 1 mM phenylmethylsulfonylfluoride (pH 7.4). Adipocytes were diluted in this medium and incubated in 60-mm sterile tissue culture dishes (1×10^5 cells/ml) for 4 h in air. To prepare liver and kidney cells, liver and kidney tissues from carp were cut into small

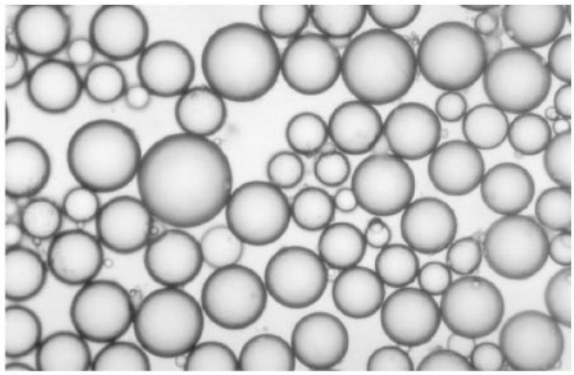

FIG. 1. Isolated carp adipocytes. Carp adipocytes were isolated by the method described in *Materials and Methods*. The cells were placed on a slide and observed through an inverted microscope (magnification, ×400; Axiovert 25, Carl Zeiss, Oberkochen, Germany).

pieces and transferred to a30-ml plastic centrifuge tube, which contained MEM (the salinity of MEM was adjusted to 0.6%). The liver and kidney fragments (1 g/10 ml medium) were incubated for 15 min at 30 C with gentle shaking (40 cycles/min) in a water bath under constant gassing with a mixture of 95% O_2-5% CO_2. This process was repeated by changing the medium so that liver and kidney fragments were properly washed and then transferred to MEM containing 0.5% collagenase. The tissues were incubated for 60 min, and aliquots were examined for the presence of isolated liver and kidney cells. Under this condition about 75% of liver tissue and 60% of kidney tissues became soft, and cells were dispersed by collagenase. The soft tissue of liver and kidney remained in the test tube, and the aliquot containing the cell suspension was collected by Pasteur pipette and transferred to a plastic tube, then centrifuged at 250 × *g*. The pellets containing cells were rewashed in MEM (without collagenase). The cell suspensions were examined for morphological integrity and viability by the exclusion of 0.1% trypan blue, and in both the cases viability was between 80–90%. Isolated liver and kidney cells were distributed among 60-mm sterile tissue culture dishes (1×10^5 cells/ml) and incubated as described above. On termination of the incubation at 4 h, aliquots from the medium of different cell incubations were subjected to insulin RIA developed with antiporcine insulin antibody raised in the laboratory of Prof. K. Wakabayashi (Gunma University, Maebashi, Japan).

Northern blot analysis

RNA was isolated using the Tri-Pure RNA extraction kit (Roche Molecular Biochemicals, Mannheim, Germany) following the manufacturer's instructions. Ten micrograms of total RNA were loaded on each lane of a 1.5% formaldehyde-agarose gel, electrophoresed, and transferred to a nylon membrane by capillary suction method (Hybond-N^+, Amersham Pharmacia Biotech, Indianapolis, IN). The membranes were hybridized by the following probes: 349-bp *Bam*HI-digested fragment of rat insulin cDNA clone present in pGEM-T vector (gift from Dr. Toshiyuki Takeuchi, Maebashi, Japan), 450-bp *Eco*RI-*Hin*dIII fragment of zebrafish insulin cDNA clone present in pBluescript vector (gift from Dr. Stephen J. Duguay, Chicago, IL), and 1.3-kb *Bam*HI-*Not*I fragment of rat flotillin cDNA clone present in pZero-2 vector (gift from Dr. Perry Bickel, St. Louis, MO). Prehybridization was allowed for 2 h in the buffer containing 6× standard saline citrate with 50% formamide, 1× Denhardt's solution, and 0.5% sodium dodecyl sulfate at 42 C. Hybridization was carried out under the same conditions with [α-^{32}P]dATP-labeled rat and zebrafish insulin cDNA fragments for 18 h. The membrane was washed for 90 min at 65 C in 2× standard saline citrate containing 0.1% sodium dodecyl sulfate with subsequent three changes of buffer. The hybridized membrane was exposed to Kodak x-ray film (Eastman Kodak Co., Rochester, NY) and kept at −80 C for 3 d. RNA molecular size markers (0.28–6.5 kb) used were purchased from Promega Corp. (Madison, WI). The digestion of DNA, agarose gel electrophoresis, random labeling of DNA, and Northern hybridization were performed as described by Sambrook *et al.* (15).

Western blot analysis

The isolated cells were homogenized in homogenizing buffer (150 mM NaCl, 500 mM Tris, and 10 mM EDTA) supplemented with protease inhibitors (1 μg/ml aprotinin, 1 μg/ml pepstatin, 1 μg/ml leupeptin, 1 mM phenylmethylsulfonylfluoride, and 1 μg/ml trypsin inhibitor) and 1% Triton X-100. It was then centrifuged at 5000 rpm for 10 min at 4 C. The supernatant was collected, and an aliquot was taken for protein assay. Protein was quantified by the method described by Lowry *et al.* (16) and then resolved on a 10% sodium dodecyl sulfate-polyacrylamide gel and transferred to Immobilon-P membranes (Millipore Corp., Bedford, MA). Membrane was incubated with 5% blocking solution (Tris-buffered saline containing 0.1% Tween 20, and 5% nonfat dried milk) for 1 h, washed twice with Tris-buffered saline containing 0.1% Tween 20 and then incubated for 16 h with rabbit anti-Glut4 (a gift from Dr. David E. James, University of Queensland, Queensland, Australia; 1:1000 dilution in 5% blocking solution), rabbit anti-Glut2, or rabbit antiperoxisomal proliferator-activated receptor γ (anti-PPARγ) antibody (both from Santa Cruz Biotechnology, Inc., Santa Cruz, CA; 1:2000 dilution in 5% blocking solution). Immunoreactive bands were visualized by reacting alkaline phosphatase-labeled secondary goat antirabbit antisera at 1:2000 dilution with the substrate nitro blue tetrazolium/5-bromo-4-chloro-3-indolyl-phosphate (15).

Confocal microscopy

To determine the localization of insulin and leptin in carp and rat adipocytes, cells were adhered on poly-L-lysine-coated slides. Thereafter, cells were fixed with 4% paraformaldehyde for 20 min at 4 C; permeabilized with permeabilization buffer (PB) containing Dulbecco's PBS without Ca^{2+} and Mg^{2+}, 1% heat-inactivated fetal calf serum, 0.1% sodium azide, and 0.1% saponin, pH 7.4–7.6; and blocked with 2% goat serum containing 0.1% sodium azide and 0.1% saponin. The cells were double-labeled with leptin rabbit polyclonal and human antiinsulin mouse monoclonal antibodies. Cells were again washed with PB and incubated with fluorescein isothiocyanate and tetramethylrhodamine isothiocyanate-conjugated goat antirabbit and antimouse secondary antibodies, respectively. After washing the cells with PB with and without saponin, PBS containing 1% paraformaldehyde without saponin was added. The cells were finally mounted in 90% glycerol. For a negative control, the cells were fixed, and immunofluorescence was conducted using only secondary antibody and without any primary antibody,. Fluorescence was examined with a TCS-SP (UV) four-channel confocal laser scanning microscope (Leica Corp., Rockleigh, NJ). The cell monolayer was optically sectioned every 0.5 μm. Image resolution using a ×63 Neofluor objective and TCS-SP software (both from Leica Corp.) was 512 × 512 pixels.

Purification of carp fat cell insulin

Fat cells were lysed by sonication in ethanol/0.7 M HCl (3:1, vol/vol) under ice and centrifuged at 5000 × *g* for 10 min at 4 C. The pH of the supernatant was adjusted to 3.0 with a concentrated ammonium solution and extracted with 4 vol diethyl ether for 20 h at 4 C. The precipitate was washed with acetone followed by ether and allowed to air-dry; this was then extracted with 1 M acetic acid and centrifuged. The supernatant was reextracted with chilled acetone and subjected to petroleum benzene extraction. The resultant precipitate was dried and extracted with chilled acetic acid (1 M). The extracted material was gel-filtered through Sephadex G-50, and an insulin-immunoreactive peak was lyophilized. This was further purified on a fast protein liquid chromatography reverse phase Pep-RPC column (Amersham Pharmacia Biotech) equilibrated with 0.1% (vol/vol) trifluoroacetic acid/water. The fractions were eluted using acetonitrile linear gradients, and the amount of protein under each peak was measured according to the method of Lowry *et al.* (16). The immunoreactive insulin peaks were pooled, lyophilized, and subjected to 5–15% gradient SDS-PAGE (17).

Insulin injection

Adipocyte immunoreactive insulin (20 μg/100 g body weight) from incubation medium or 10 μg/100 g body weight AdpInsl (purified adipocyte insulin) or porcine insulin was ip injected into the strepto-

zotocin-treated male Sprague Dawley rats, weighing 100–150 g. After 6 h of injection, blood was collected by retroorbital puncture using a capillary tube and centrifuged to collect plasma. Its glucose content was determined by the glucose-glucose oxidase method (glucose test kit, Span Diagnostic, Surat, India).

Determination of insulin activity in vitro

Freshly prepared adipocytes were suspended in MEM, and after 2 h 1.0 μCi D-[^{14}C]glucose was added to the adipocyte incubation. AdpInsl or porcine insulin (25 ng/ml) was added to the incubation, and glucose uptake was measured according to a previously described method (18). The initial rate of glucose uptake was determined from the incubation of adipocyte without insulin. The reaction was stopped at 5 min (optimum time selected from the time kinetic study) by washing the cells three times with ice-cold MEM in the presence of 0.3 mM phloretin to correct the glucose uptake data from simple diffusion and nonspecific trapping of radioactivity.

RT-PCR, subcloning, and sequencing

Insulin gene fragments were isolated from carp fat cell RNA using RT-PCR. First strand cDNA synthesis was carried out with 10 μg total RNA using Superscript II RT (Life Technologies, Inc., Grand Island, NY) enzyme. Oligo(deoxythymidine) primer (5′-GGAAGCTTTTTTTTT-TTTTTTTTTT-3′), 10 μM dithiothreitol, 0.5 mM of each deoxynucleoside 5′-triphosphate, and the buffer supplied with the enzyme [containing 50 mM Tris-HCl (pH 8.3), 75 mM KCl, and 3 mM $MgCl_2$] were added to the RT reaction mixture (final volume, 20 μl) and incubated at 42 C for 1 h. A 100-μl PCR volume was made by adding 2.5 U *Taq* DNA polymerase (Life Technologies, Inc.), to a PCR mixture containing 1× reaction buffer [50 mM KCl, 10 mM Tris-HCl (pH 8.3), 0.1% Triton X-100, and 2.5 mM $MgCl_2$], and 200 μM of each deoxy-NTP (Sigma-Aldrich), 4 μM of each primer (sense and antisense), and a 5-μl aliquot from the RT reaction mixture. The sense oligonucleotide primers (SB1, 5′-GGGAATTCCAG-CACCTGTGTGGATC-3′; SB2, 5′-GGGAATTCGTGACCATGGCAGT-3′) were constructed on the basis of homologous domains of the preproinsulin gene sequences of different fish species as mentioned in the text. The PCR was performed for 35 cycles of denaturation at 94 C for 45 sec (5 min in the first cycle), annealing at 50 C for 45 sec, and extension at 72 C for 1 min (10 min in the last cycle; Perkin-Elmer 9700, PE Applied Biosystems, Foster City, CA). As the enzyme-recognizable sequences *Eco*RI and *Hin*dIII were tagged to the 5′ termini of the sense primers and antisense primer oligo(deoxythymidine), respectively, the RT-PCR products were digested by those enzymes. The digests were electrophoresed on 1.5% agarose gel; the band was excised and purified using a QiaEx-II gel extraction kit (QIAGEN, Hilden, Germany). It was then cloned directionally into the pBluescript plasmid vector (Stratagene) in *Eco*RI-*Hin*dIII site. Sequencing of the RT-PCR product was performed using a PRISM dye system (Perkin-Elmer, PE Applied Biosystems) automated sequencer. Amino acid and nucleic acid sequences of different organisms were collected from the NCBI database.

5′ Rapid amplification of cDNA ends (5′ RACE) of insulin gene

To obtain the 5′ untranslated region (UTR) of the insulin gene, the 5′ RACE technique was used. Rat adipocyte RNA was isolated as described above and used for 5′ RACE of the insulin gene using the Life Technologies, Inc. kit following the manufacturer's instructions. The gene-specific primers used for the RT were 5′-CC AAG CTT ACG TCT CTC TTG GGG TTG TA-3′ for the first strand cDNA synthesis, 5′-GGG ATCCCT TGG GGT TGT AGA AGA A-3′ for PCR of dC-tailed cDNA with abridged anchor primer (AAP, supplied with the kit), and 5′-CC AAG CTT ACC AGC CTG GAG CCA CAC TG-3′ for the nested amplification with the abridged universal amplification primer (AUAP, supplied with the kit). The RACE product was cloned and sequenced following the methods described above.

Computational tools and hardware

Predictions of three-dimensional structures were made by knowledge-based homology modeling using InsightII 98.0 of MSI (Biosym Technologies, San Diego, CA), ABGEN (19), and our in-house package of MODELYN and ANALYN (20) in UNIX as well as in the MS Windows environment. Energy minimization and molecular dynamics were performed with the InsightII 98.0/Discover package using the cff91 force field on a Silicon Graphics OCTANE workstation. Energy minimizations were made with a convergence criterion of 0.001 kcal/mol, using a combination of steepest descent and conjugate gradient methods (100 steps each); these steps were repeated until satisfactory conformational parameters were obtained. Molecular dynamics simulations were carried out using a time step of 1 fsec for 100 steps of equilibration and 1000 steps of dynamics. Distance constraints were applied to the other parts of the molecule while running minimization and dynamics for regularization of selected segments. The electrostatic potential surfaces of the proteins were determined by MOLMOL (21). PROCHECK (22) was used for checking the structural parameters and comparing with reference protein structures.

Results

Immunoreactive and bioactive insulin from adipocytes

We were puzzled to find a high amount of immunoreactive insulin (ir-insulin) in carp plasma without the existence of principal islet tissues. This led us to make a thorough search of different tissues for detecting the source of the circulatory insulin. Surprisingly, adipocytes showed localization of ir-insulin (Fig. 2), suggesting that these cells may secrete insulin. To examine this, we isolated adipocytes, incubated them *in vitro*, and then checked the medium for detecting ir-insulin. Figure 3A shows that adipocytes secrete considerable amounts of ir-insulin, whereas the medium from hepatocytes and kidney cells did not show the presence

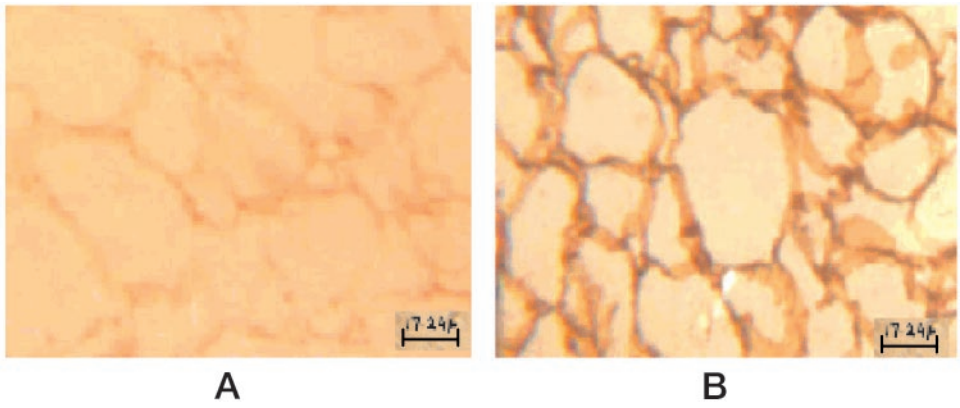

FIG. 2. Immunocytochemistry of adipocytes showing the presence of insulin in control (A) and experimental (B) sets. Paraffin-embedded fat tissue was incubated with (B) or without (A; control) porcine insulin antibody (20 μg/ml) after 15-min incubation with 0.6% H_2O_2 (vol/vol) in 80% methanol and then 45-min incubation with rabbit antiguinea pig immunoglobulin-horseradish peroxidase (diluted 1:100, vol/vol, in 10% PBS). The reaction was developed using a freshly prepared solution of 0.05% (wt/vol) diaminobenzidene and 0.03% H_2O_2 in PBS.

of ir-insulin, indicating specificity of this secretion. The bioactivity of this ir-insulin was examined by injecting the adipocyte extract or incubation medium into the rat. Both significantly reduced plasma glucose level (Fig. 3B). Glucose is a known agonist of insulin secretion from pancreatic β-cells. When the concentration of glucose was increased approximately 10 times in the incubation medium, insulin release from adipocytes was stimulated to more than 2-fold (Fig. 4A), suggesting glucose-dependent insulin secretion. To obtain this response, glucose transport to pancreatic β-cells was performed by Glut2, an isoform of the glucose transporter. Glut2 was detected in carp adipocyte (Fig. 4B). To confirm the identity of these cells as adipocytes, we examined the following criteria: 1) the expression of the adipocyte-specific gene flotillin, 2) the presence of PPARγ, and 3) the presence of Glut4. We used the mouse flotillin cDNA probe for Northern hybridization with carp adipocyte RNA. Figure 5A(a) shows hybridization signal with adipocyte RNA, whereas RNA from carp muscle, liver, and kidney did not produce any signal (data not shown). The hybridized transcript size was approximately 1.9 kb. Increasing amounts of adipocyte extract produced greater cross-reaction with PPARγ antibody [Fig. 5A(b)]. The presence of Glut4 is a characteristic of insulin target cells; as the adipocyte is one such cell, its identification in carp adipocytes [Fig. 5A(c)] distinguished them from pancreatic β-cells. Although Glut4 is not a specific marker for adipocytes, its presence distinguished them from pancreatic β-cells, which lack Glut4. The most convincing evidence in favor of adipocyte's secretion of insulin was obtained from the colocalization of leptin and insulin using dual immunofluorescence staining. Confocal microscopy showed the localization of the adipocyte-specific protein leptin and insulin in the same cell [Fig. 5B(a–d)]. Rat adipocytes, on the other hand, lacked insulin localization, indicating localization of insulin as a special attribution of adipocytes [Fig. 5B(e)].

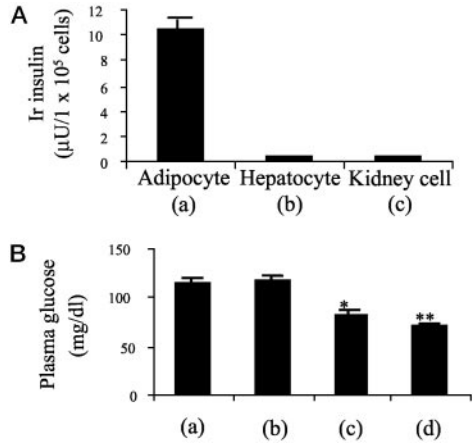

FIG. 3. Immunoreactive and bioactive insulin from carp adipocytes. Adipocytes, hepatocytes, and kidney cells were isolated and incubated *in vitro* in the manner described in *Materials and Methods*. A, Medium was collected on termination of incubation of adipocytes (a), liver cells (b), and kidney cells (c) and subjected to insulin RIA. Each value is the mean ± SEM of 10 observations. B, Rats were injected with 50 μg protein from adipocyte extract (c) or 20 μg protein from the incubation medium with adipocytes (d) or only medium (b) or without any injection (a). Blood was collected at 6 h, and glucose content was determined. Each value is the mean ± SEM of six independent determinations. *, $P < 0.05$; **, $P < 0.01$ (compared with a and b).

To purify insulin from the adipocyte, cells were lysed by sonification, followed by solvent fractionation, gel permeation chromatography, and fast protein reverse phase chromatography. Purified AdpInsl comigrated with porcine and bovine insulin in SDS-PAGE, indicating the similarity of their molecular sizes (~5.5 kDa; Fig. 6). Injection of AdpInsl to streptozotocin-induced diabetic rats significantly reduced hyperglycemia ($P < 0.001$). Its hypoglycemic activity was 25% greater than that of porcine insulin (Fig. 7A). AdpInsl stimulated a more than 2-fold increase in glucose uptake by carp and hamster adipocytes; its stimulation was significantly higher ($P < 0.05$) than that of porcine insulin [Fig. 7B(b and c)].

Insulin gene expression in adipocytes and cloning of AdpInsl

The most important question is whether adipocytes can express the insulin gene. To resolve this, we used an insulin cDNA probe from rats and zebrafish for Northern hybridization with carp adipocyte RNA. Figure 8A shows hybridization of carp adipocyte RNA with zebrafish and rat insulin cDNA, whereas hybridization signal was not detected with adipocyte RNA from rat, guinea pigs and hamsters (Fig. 8B). The size of the hybridized transcript was about 700 bp, which is close to that of the pancreatic β-cell insulin gene. To characterize the AdpInsl gene, a consensus oligonucleotide primer (SB-1) was designed from selected homologous domains of preproinsulin cDNA from zebrafish (*Danio rerio*, GenBank accession no. AF036326), European carp (*Cyprinus carpio*, GenBank accession no. X00989), salmon (*Onchorynchus keta*, GenBank accession no. L11712), and tilapia (*Tilapia*

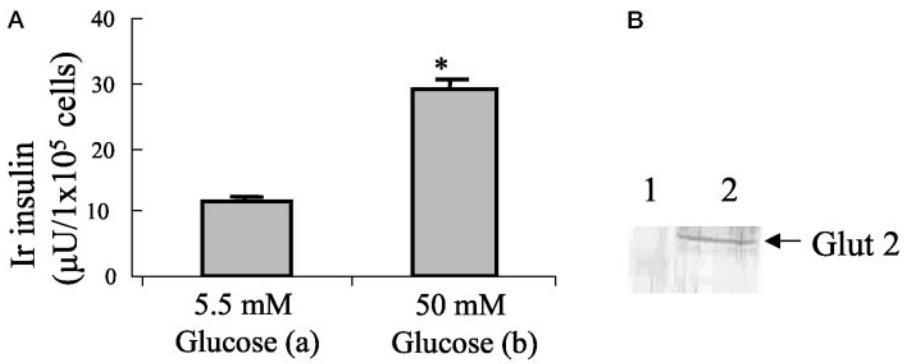

FIG. 4. A, Glucose-dependent insulin secretion from adipocytes. The amount of ir-insulin released by carp adipocytes in the medium containing 5.5 mM glucose (a) and 50 mM glucose (b). B, Presence of Glut2 in the adipocyte. Total protein (adipocyte cell extract; 100 μg) was subjected to SDS-PAGE (lane 2), transferred to a polyvinylidene difluoride membrane, and probed with anti-Glut2 antibody. Molecular size markers were loaded on lane 1. *, $P < 0.001$.

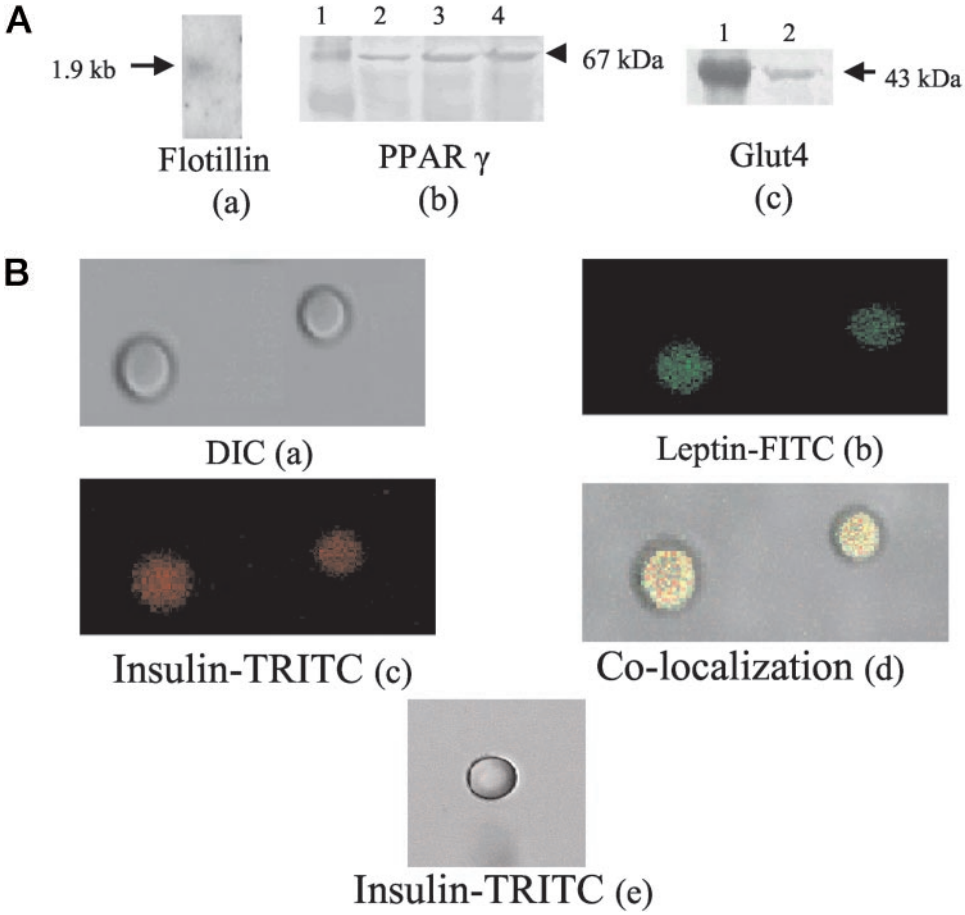

FIG. 5. A, Expression of adipocyte-specific markers. a, Adipocyte RNA (10 μg) was loaded and probed with radiolabeled flotillin cDNA. b, Ten, 20, and 30 μg total protein (adipocyte cell extract) was run on SDS-PAGE (lanes 2, 3, and 4, respectively) with molecular size markers (lane 1), transferred onto a polyvinylidene difluoride membrane, and probed with anti-PPARγ antibody. c, Total protein (adipocyte cell extract; 25 μg) was loaded on SDS-PAGE (lane 2), transferred onto a polyvinylidene difluoride membrane, and probed with anti-Glut4 antibody. Molecular size markers were loaded on lane 1. B, High magnification confocal fluorescence microscopy of adipocytes. Confocal microscopy of the adipocytes was performed on a layer of cells adhered on poly-L-lysine-coated slides. The fixed, permeabilized, and blocked cells were double labeled with leptin rabbit polyclonal and human antiinsulin mouse monoclonal antibodies. The secondary antibodies used were fluorescein isothiocyanate- and tetramethylrhodamine isothiocyanate-conjugated antirabbit and antimouse secondary antibodies. a, Differential interference contrast (DIC) showing carp adipocytes; b, carp adipocytes showing the expression of leptin; c, carp adipocytes showing the expression of insulin; d, colocalization of leptin and insulin; e, rat adipocyte stained with human antiinsulin mouse monoclonal primary antibody and TRITC-conjugated goat antimouse secondary antibody.

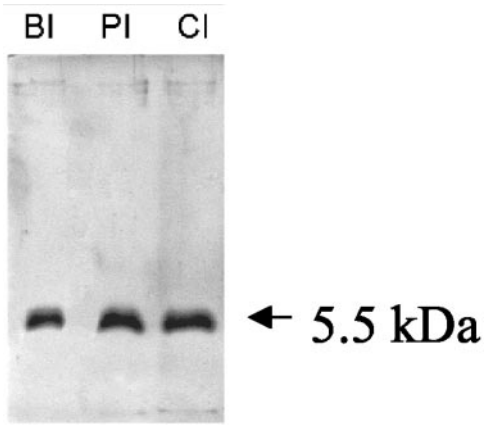

FIG. 6. Comigration of purified carp fat cell insulin (CI) with bovine (BI) and porcine (PI) insulin. Five micrograms of each insulin were subjected to 5–15% gradient SDS-PAGE, followed by Coomassie Blue staining.

nilotica, GenBank accession no. AF038123). RT-PCR performed with adipocyte total RNA produced a 375-bp DNA fragment using SB1 and oligo(deoxythymidine) primers. This product was cloned and sequenced. Nucleotide sequence analysis of this clone showed more than 90% positional homology with the preproinsulin gene of zebrafish. The amplified and sequenced portion of cDNA corresponded to AdpInsl A and C peptide regions, but lacked 5′ sequences of cDNA corresponding to the B chain. As the B chain of AdpInsl could not be sequenced with the SB1 primer, another primer, SB2, was synthesized on the basis of the *Danio* signal peptide sequence. This was expected to give the full sequence of the B chain. Utilization of SB-2 and oligo(deoxythymidine) primers in RT-PCR produced a 425-bp DNA fragment. The amplified DNA fragment was cloned. Sequencing of this clone revealed complete AdpInsl signal peptide and complete 3′ UTR (Fig. 9A; GenBank accession no. AF373021). Deduced amino acid residues of AdpInsl exhibited striking homology with pancreatic β-cell insulin of different vertebrates (Fig. 9B). Its A and B chains showed 98% homology with zebrafish and more than 70% homology with human, pig, and rat insulin, although there was very little homology at the nucleotide level. To obtain the 5′ UTR, 5′ RACE was performed using the primers mentioned in *Materials and Methods*. The RACE product was cloned and sequenced. This sequence shows strong homology with the zebrafish 5′ UTR sequence.

Three-dimensional structural modeling of AdpInsl: comparison between AdpInsl and human insulin

We predicted the structure of AdpInsl from the known structure of human insulin (14) based on the sequence alignment shown in Fig. 9B. Mutations were made on each of the six monomers containing A and B chains of the nuclear magnetic resonance-derived structure, followed by place-

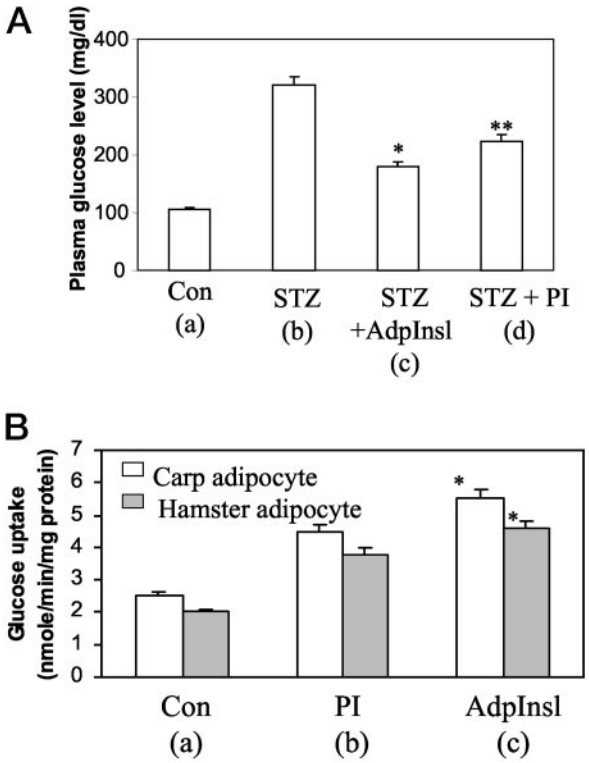

FIG. 7. A, Determination of biological activity of AdpInsl in streptozotocin-induced diabetic rats. The male Sprague Dawley rats (100–150 g body weight) were selected for streptozotocin (STZ) treatment; 55 mg/kg STZ were injected ip into the rat, and those animals exhibiting 250–320 mg glucose/100 ml blood in the third week of injection were taken for experiments. a, Rats not treated with STZ, only vehicle (0.9% saline; n = 6); b, STZ- and vehicle-injected rats (n = 6); c, STZ-treated rat injected with AdpInsl; d, STZ-treated rat injected with porcine insulin (PI; 10 μg AdpInsl or PI wre injected/100 g body weight). Each value is the mean ± SEM of six observations. *, $P < 0.001$, c compared with b; **, $P < 0.05$, c compared with d. B, Effects of PI (b), AdpInsl (c), and vehicle (a) on glucose uptake by carp and hamster adipocytes. Adipocytes (1×10^5 cells/incubation) were suspended in MEM containing 1% fetal calf serum and preincubated for 2 h in the absence of insulin; after the addition of D-[^{14}C]glucose, uptake by the cells was determined by the procedure described in *Materials and Methods*. *, $P < 0.05$, AdpInsl compared with PI.

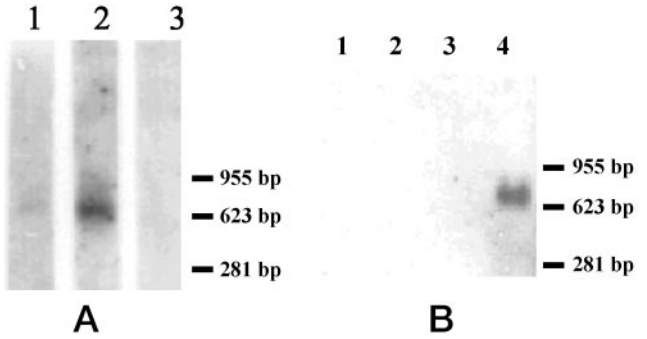

FIG. 8. Expression of the insulin gene in adipocytes. A, Ten micrograms each of total carp adipocyte RNA (lanes 1 and 2) and carp kidney RNA (lane 3) were electrophoresed and transferred onto a Nytran membrane. The membrane was then probed with rat insulin cDNA (lane 1) and zebrafish insulin cDNA (lane 2 and 3). B, Ten micrograms each of total RNA from adipocytes of rat (lane 1), guinea pig (lane 2), hamster (lane 3), and carp (lane 4) were electrophoresed and transferred onto a Nytran membrane. The membrane was then probed with zebrafish insulin cDNA.

ment of the side-chains with minimum bumps with the surrounding atoms. The resulting hexameric structure was energy-minimized. A monomer was separated to examine the effect of mutation and to map the electrostatic potential on its surface, as the monomer is the receptor-binding unit.

Alanine scanning mutagenesis of insulin showed that receptor binding is very strongly affected by mutations at Gly-B23 and Phe-B24 of the B chain and at Ile-A2, Val-A3, and Tyr-A19 of the A chain. These amino acids (Fig. 9B, *red*) have been colored red in the structures of both the AdpInsl (Fig. 10A) and human (Fig. 10B) insulins. Some other amino acids that are known to affect the receptor binding to some extent (Fig. 9B, *pink*) are then oriented in such a way that the receptor-binding regions are placed at the front (inside the *yellow* ring, Fig. 10, A and B). It is noteworthy that although the AdpInsl differs from its human counterpart in the number of amino acids in both chains (Fig. 9), the strategically important amino acids provide strikingly similar structural motifs, differing by only one amino acid, *i.e.* at the eighth position of the A chain (His in AdpInsl and Thr in human insulin; Fig. 9). The side-chain of the His-A8 residue points along the surface of the helix, making the N-terminal α-helix more stable, which was also demonstrated by nuclear magnetic resonance studies on an engineered variant of human insulin. This change favored receptor binding by 43% (12). Figure 10, C (AdpInsl) and D (human insulin), show the electrostatic potential at these surfaces, which are probably the complementary regions in the ligand-receptor interface. The central parts of these surfaces in both AdpInsl and human insulins are neutral, indicating the dominance of hydrophobic forces in receptor binding. There is a slight difference at the *upper right corner* of the *yellow* ring where AdpInsl is basic (Fig. 10C), but human insulin is acidic (Fig. 10D), in nature.

Discussion

We have serendipitously discovered carp adipocyte as an exceptional cell in which the insulin gene is expressed, and protein is secreted. To prove the identity of this cell, we have used adipocyte-specific expression of the flotillin gene, leptin, and PPARγ proteins as markers. Colocalization of insulin and leptin strengthens the special attributions displayed by these cells. Although the presence of insulin has been shown in certain invertebrates (3) and in the extrapancreatic tissues of rats and humans (4), the expression of the insulin gene and the secretion of insulin are still known to be pancreatic β-cell specific. Carp adipocyte is a unique cell; on the one hand, it is functionally similar to the pancreatic β-cell, and, on the other hand, it possesses the characteristics of a fat cell, an insulin target cell. Like the pancreatic β-cell, the carp adipocyte responds to glucose challenge, and the presence of Glut2 as s transporter shows that the existence of a glucose sensor is required for glucose-dependent insulin secretion. To date no other naturally occurring cell showed such a functional duality. Our investigation shows that purified AdpInsl from carp adipocytes is structurally and functionally very similar to pancreatic β-cell insulin. AdpInsl has 98%

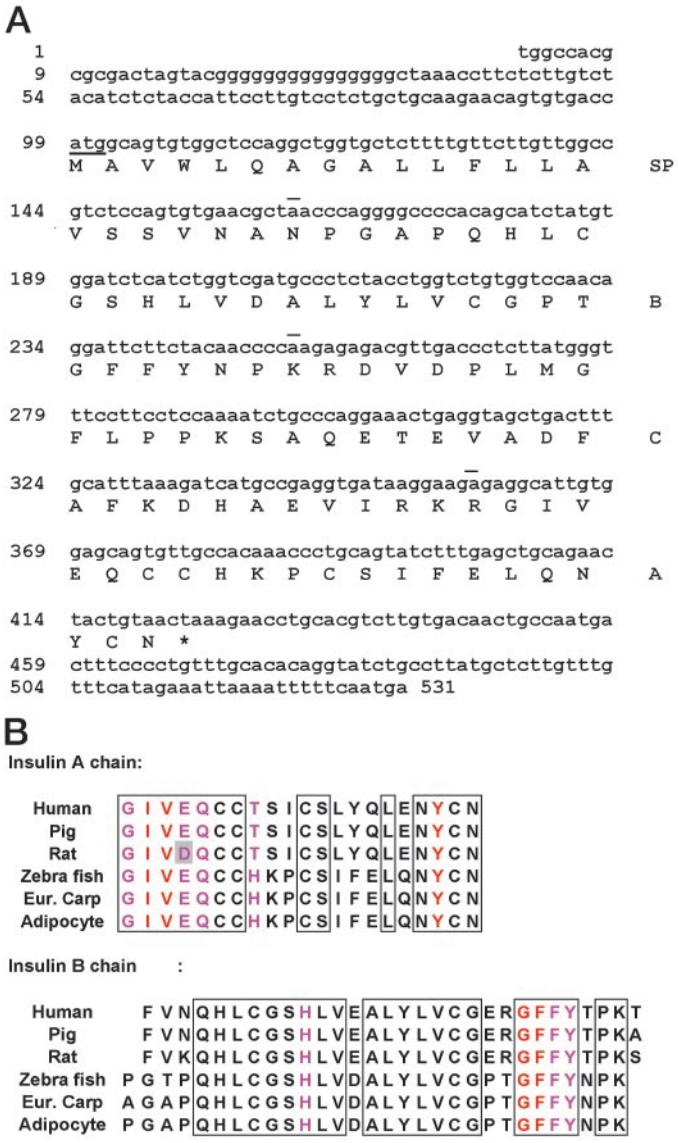

FIG. 9. A, Nucleotide and the deduced amino acid sequences of the preproinsulin gene of carp showing signal peptide (SP; 1–22 amino acids) and B (23–52 amino acids), C (53–87 amino acids), and A (88–108 amino acids) chains. The 5′UTR and 3′UTR sequences are also shown. The *lowercase letters* represent the nucleic acid sequence, and the amino acids are represented by *uppercase letters*. The start codon is *underlined*, and the stop codon is indicated by an *asterisk*. The probable cleavage sites between the signal peptide and B, between B and C, and between C and A are represented by *vertical arrows*. B, Comparison of the predicted amino acid sequences of insulin A and B chains of human, rat, pig, zebrafish, and European carp and adipocytes of Indian carp. Their positional homologies were examined. The *box* represents the homologous domains, whereas the *shaded letter in the box* shows the nonidentical amino acid. Mutations of the residues colored in *red* are the most disruptive mutations (to Ala) in terms of receptor binding of human insulin in the A chain, and other amino acids that are known to be involved in the receptor binding are colored *pink* in the B chain (12, 13).

homology with zebrafish β-cell insulin and more than 70% homology with porcine and human insulins. If we consider the peptide segments of insulin involved in transducing signals by recognizing the surface receptor molecule, they remain far more conserved than the total peptide chains.

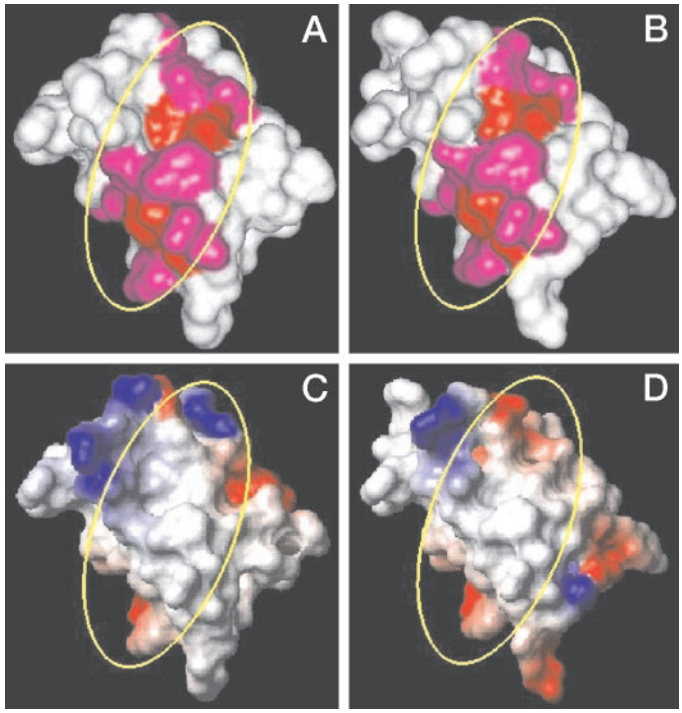

FIG. 10. A, The connolly surface of the modeled monomer of AdpInsl calculated using InsightII. Residues Gly-B23, Phe-B24, Ile-A2, Val-A3, and Tyr-A19, which are strongly implicated in receptor binding, as evidenced by different experimental techniques, are colored *red*, and some other amino acids, Phe-B25, Tyr-B26, His-B10, Gly-A1, Glu-A3, Gln-A4, and His-A8, that are known to affect receptor binding to some extent are colored *pink*. The structure was oriented in such a way that the highly potential receptor binding surface is fully exposed (within the *yellow* band). B, The connolly surface of the reference human monomer in the same orientation with the same color convention (only exception is that the amino acid at the A8 position is Thr instead of His in AdpInsl). C and D, The same surfaces as in A and B, respectively, but colored according to the electrostatic potential of the surface and calculated using MOLMOL. The *blue* color depicts the positively charged basic regions, the *red* color shows the negatively charged acidic regions, and the *white* color is for the neutral hydrophobic regions. Regions of intermediate colors arise due to the net result of mixed electrostatic potentials.

AdpInsl is from the carp adipocyte, which is a lower vertebrate; even there the critical determinant segment for receptor binding is highly homologous to mammalian insulin. It is interesting that there is about a 30% difference in the amino acids of the A and B chains between human and AdpInsl, but the biological function of this key hormone remains well conserved. Although there is a considerable homology in the sequence of amino acid between AdpInsl and mammalian insulin, it is not so at the nucleotide level, as different codons have been used for the same amino acid. About 85% nucleotides in AdpInsl and zebrafish insulin are different from mammalian insulin, indicating a change in genetic make-up in the evolution of this molecule, keeping the peptide structure more conserved. Although the amino acid sequence of AdpInsl has about 70% homology with human, porcine, and rat insulin, their codon usage varied widely, as only about 15% of the nucleotides are common. AdpInsl has strongest homology with zebrafish β-cell insulin, 98% in peptide structure and more than 90% in nucleotide sequence. This is the

reason for the strong hybridization signal with zebrafish insulin cDNA and the weak signal with rat insulin cDNA.

Functionally, AdpInsl is more active than porcine insulin in rats. Injection of AdpInsl into the streptozotocin-induced diabetic rat produced significantly stronger hypoglycemic effect compared with porcine insulin. AdpInsl stimulated glucose uptake by adipocytes more actively than porcine insulin not only in carp adipocytes, but also in hamster adipocytes. All of these indicate a better recognition of the insulin receptor in mammalian targets by AdpInsl compared with porcine insulin. This prompted us to compare the peptide segment of AdpInsl with porcine and human insulin in relation to receptor interactions. The A1-A8 sequence (GIVEQCCT) of porcine and human insulin contains critical determinants of receptor binding. The importance of this segment in insulin receptor interactions was recognized early by measuring the biological activity for various derivatives (23, 24). The A1-A8 sequence has low intrinsic helical propensities and an unfavorable C-cap residue (Thr^8) (25). Any substitution between A1-A3 amino acid residues is detrimental to biological activity (26, 27). On the other hand, substitution of His or Arg for Thr (8) exhibits a significant increase in activity (28) in accordance with the thermodynamic stabilization with an enhancement of the folding stability (29). It has been demonstrated that the mutation of A8 from Thr^8 to His (8) or Arg^8 in an engineered insulin resulted in a 43% increase in its receptor binding affinity. AdpInsl has His^8, a favorable substitute against unfavorable Thr^8 in human and porcine insulin; this is the reason for its greater biological activity. Moreover, the most important segment of insulin peptide related to the receptor binding includes A1-A4, A19, B12, and B24-B26 (12), and AdpInsl has all of these segments in position.

Recent reports show that fat cells are not merely a storage depot for triglycerides; they are highly active endocrine cells, sensing metabolic signals and secreting hormones that regulate energy homeostasis (30–32). The adipocyte appears to be the prime cell dealing with insulin resistance and type 2 diabetes; adiponectin and PPARγ can reverse insulin resistance by reducing triglyceride levels in insulin target organs (33–35). Lipodystrophies produce insulin resistance, and transplantation of adipose tissue into lipoatrophic diabetic mice dramatically reverses hyperglycemia by improving muscle insulin sensitivity (36). Carp adipocytes possess similar characteristics as mammalian adipocytes in having PPARγ, leptin, flotillin, and Glut4; in addition, they can express the insulin gene and secrete insulin protein and therefore can deliver insulin to maintain glucose homeostasis. Hence, the carp adipocyte is promising for future therapy of type 2 diabetes and insulin resistance that would require successful transfer of these cells to the host by a suitable engineering technique.

Acknowledgments

We gratefully acknowledge the gift of rat insulin cDNA from Dr. Toshiyuki Takeuchi (Gunma University Institute for Molecular and Cellular Regulation, Maebashi, Japan), the gift of zebrafish insulin cDNA from Dr. Stephen J. Duguay (Howard Hughes Medical Institute Research Laboratories, University of Chicago, Chicago, IL), and the gift of flotillin cDNA from Dr. Perry Bickel (Washington University School of Medicine, St. Louis, MO). We deeply appreciate Dr. P. Roy (Imperial College Faculty of Medicine, London, UK) for his help with the leptin antibody (Santa Cruz Biotechnology, Inc., Santa Cruz, CA). We also acknowledge Dr. Gayatri Tripathi for confocal microscopy, and Mr. Swapan Mondal (Indian Institute of Chemical Biology, Calcutta, India) for helping us with the insulin RIA.

Received March 26, 2002. Accepted December 12, 2002.

Address all correspondence and requests for reprints to: Prof. Samir Bhattacharya, Indian Institute of Chemical Biology, 4 Raja S. C. Mullick Road, Calcutta 700032, India. E-mail: samir@iicb.res.in.

This work was supported by a research grant from the Department of Biotechnology, Ministry of Science and Technology (New Delhi, India; BT/PR1652/AAQ/03/081/99) and a grant from the Council of Scientific and Industrial Research (New Delhi, India) to this institute.

* S.S.R., M.M., and S.B. contributed equally to this study.

References

1. **Le Roith D, Shiloach J, Heffron, R, Rubinovitz C, Tanenbaum R, Roth, J** 1985 Insulin-related material in microbes: similarities and differences from mammalian insulins. Can J Biochem Cell Biol 63:839–849
2. **Le Roith D, Shiloach J, Lesniak, MA** 1980 Evolutinary origins of vertebrate hormones: substances similar to mammalian insulins are native to unicellular eukaryotes. Proc Natl Acad Sci USA 77:6184–6188
3. **Le Roith D, Lesniak MA, Roth J** 1981 Insulin in insects and annelids. Diabetes 30:70–76
4. **Rosenzweig JL, Havrankova J, Lesniak MA, Brownstein M, Roth J,** Insulin is ubiquitous in extrapancreatic tissues of rats and humans. Proc Natl Acad Sci USA 77:572–576
5. **Muglia L, Locker J** 1984 Extrapancreatic insulin gene expression in the fetal rat. Proc Natl Acad Sci USA 81:3635–3639
6. **Plisetskaya EM** 1989 Physiology of the fish endocrine pancreas. Fish Physiol Biochem 7:39–48
7. **Epple A, Lewis TL** 1973 Comparative histophysiology of the pancreatic islets. Am Zool 13:567–590
8. **Youson JH, Al-Mahrouki** 1999 Ontogenic and phylogenic development of the endocrine pancreas (islet organ) in fishes. Gen Comp Endocrinol 116:303–335
9. **Mommsen TP, Plisetskaya EM** 1991 Insulin in fishes and agnathan: history, structure, and metabolic regulation. Rev Aquatic Sci 4:225–359
10. **Humbel RE, Bosshard HR, Zahn H** 1972 Chemistry of insulin. In: Steiner DF, Freinkel N, eds. Handbook of physiology, vol 1. Baltimore: Williams & Wilkins; 111
11. **Cosmatos A, Cheng K, Okada Y, Katsoyannis PG** 1978 The chemical synthesis and biological evaluation of [1-L-alanine-A]-and [1-D-alanine-A]insulins. J Biol Chem 253:6586–6590
12. **Olsen HB, Ludvigsen S, Kaarsholm NC** 1998 The relationship between insulin bioactivity and structure in the NH_2-terminal A-chain helix. J Mol Biol 284: 477–488
13. **Kristensen C, Kjeldsen T, Wiberg FC, Schaffer L, Hach M, Havelund S** 1997 Alanine scanning mutagenesis of insulin. J Biol Chem 272:12978–12983
14. **O'Donoghue SI, Chang X, Abseher R, Nilges M, Led JJ** 2000 Unraveling the symmetry ambiguity in a hexamer: calculation of the R6 human insulin structure J Biomol NMR 16:93–108
15. **Sambrook J, Fritsch EF, Maniatis T** 1989 Molecular cloning: a laboratory manual. 2nd ed. Cold Spring Harbor, NY: Cold Spring Harbor Laboratory Press
16. **Lowry OH, Rosebrough NJ, Farr AE, Randall RJ** 1951 Protein measurement with the Folin phenol reagent. J Biol Chem 193:265–275
17. **Laemmli UK** 1970 Cleavage of structural proteins during the assembly of the head of bacteriophage T4. Nature 27:680–685
18. **Marshall S, Bacote V, Traxinger RR** 1991 Discovery of a metabolic pathway mediating glucose-induced desensitization of the glucose transport system. Role of hexosamine biosynthesis in the induction of insulin resistance. J Biol Chem 266:4706–4712
19. **Mandal C, Kingery BD, Anchin JM, Subramanium S, Linthicum DS** 1996 ABGEN: a knowledge-based automated approach for antibody structure modeling. Nat Biotechnol 14:323–328
20. **Mandal C** 1998 MODELYN: a molecular modeling program version PC-1.0. Indian copyright no. 9/98
21. **Koradi R, Billeter M, Wuthrich K** 1996 MOLMOL: a program for display and analysis of macromolecular structures. J Mol Graph 14:29–32, 51–55
22. **Laskowski RA, MacArthur MW, Moss DS, Thornton JM** 1993 PROCHECK: a program to check the stereochemical quality of protein structures. J Appl Cryst 26:283–291
23. **Geiger R, Geisen K, Regitz G, Summ HD, Langner D** 1980 Insulin analogoues with substitution of A1-glycine by D-amino acids and omega-amino acids. Hoppe-Seyler Z Physiol Chem 361:563–570
24. **Geiger R, Geisen K, Summ HD** 1982 Exchange of A1-glycine in bovine insulin with L- and D-tryptophan. Hoppe-Seyler Z Physiol Chem 363:1231–1239

25. **Baker EN, Blundell TL, Cutfield JF, Cutfield SM, Dodson EJ, Dodson GG, Hodgkin DMC Hubbard RE, Isaacs NW, Reynolds CD, Sakabe K, Sakabe N, Vijayan NM** 1988 The structure of 2Zn pig insulin crystals at 1.5A resolution. Phil Trans R Soc Ser B Biol Sci 319:369–456
26. **Nakagawa SH, Tager HS** 1992 Importance of aliphatic side chain structure at positions 2 and 3 of the insulin A chain in insulin-receptor interactions. Biochemistry 31:3204–3214
27. **Weiss A, Wan Z, Zhao M, Chu YC, Nakagawa SH, Burke GT, Jia W, Hellmich R, Katsoyannis PG** 2002 Non-standard insulin design: structure-activity relationships at the periphery of the insulin receptor. J Mol Biol 315:103–111
28. **Märki F, Gasparo MD, Eisler K, Kamber B, Riniker B, Rittel W, Sieber P** 1979 Synthesis and biological activity of seventeen analogues of human insulin. Hoppe-Seyler Z Physiol Chem 360:1619–1632
29. **Kaarsholm NC, Norris K, Jorgensen RJ, Mikkelsen J, Ludvigsen S, Olsen OH, Sorensen AR, Havelund S** 1993 Engineering stability of the insulin monomer fold with application to the structure-activity relationship. Biochemistry 32:10773–10778
30. **Mohamed-Ali, V, Pinkney, JH, Coppack, SW** 1998 Adipose tissue as an endocrine and paracrine organ. Int J Obes Relat Metab Disord 22:1145–1158
31. **Havel, PJ** 2000 Role of adipose tissue in body-weight regulation: mechanism regulating leptin production and energy balance. Proc Nutr Soc 59:359–371
32. **Ahima RS, Flier JS** 2000 Adipose tissue as an endocrine organ. Trends Endocrinol Metab 11:327–332
33. **Shulman GI** 2000 Cellular mechanisms of insulin resistance. J Clin Invest 106:171–176
34. **Yamauchi T, Kamon J, Waki H, Terauchi Y, Kubota N, Hara K, Mori Y, Ide T, Murakami K, Tsuboyama-Kasaoka N, Ezaki O, Akanuma Y, Gavrilova O, Vinson C, Reitman ML, Kagechika H, Shudo K, Yoda M, Nakano Y, Tobe K, Nagai R, Kimura S, Tomita M, Froguel P, Kadowaki T** 2001 The fat-derived hormone adiponectin reverses insulin resistance associated with both lipoatrophy and obesity. Nat Med 7:941–946
35. **Berg AH, Combs TP, Du X, Brownlee M, Scherer PE** 2001 The adipocyte-secreted protein Acrp30 enhances hepatic insulin action. Nat Med 7:947–953
36. **Gavrilova O, Marcus-Samuels B, Graham D, Kim JK, Shulman GI, Castle AL, Vinson C, Eckhaus M, Reitman ML** 2000 Surgical implantation of adipose tissue reverses diabetes in lipoatrophic mice. J Clin Invest 105: 271–278